Inorg. Chem. **2001,** *40,* 7014−7019

Reactions of the Protonated Dinuclear Ruthenium Complex $[\{(\eta^5\text{-}C_5H_3)_2(SiMe_2)_2\}Ru_2(CO)_4(\mu\text{-}H)]^+$ with Nucleophiles

Maxim V. Ovchinnikov, Arkady M. Ellern,[†] Ilia A. Guzei,[†,‡] and Robert J. Angelici*

Department of Chemistry, Iowa State University, Ames, Iowa 50011

Received June 18, 2001

Complex $[\{(\eta^5\text{-}C_5H_3)_2(SiMe_2)_2\}Ru_2(CO)_4(\mu\text{-}H)]^+BF_4^-$ ($\mathbf{1}H^+BF_4^-$), which features a protonated Ru−Ru bond, reacts with F^- to give $(\eta^5\text{-}C_5H_5)_2Ru_2(CO)_4$ (**2**), resulting from the cleavage of both $SiMe_2$ groups, with I^- to give the Ru−Ru cleaved product $\{(\eta^5\text{-}C_5H_3)_2(SiMe_2)_2\}Ru_2(CO)_4(H)(I)$ (**3**), and with phosphines (PEt_3, PMe_2Ph) to give $[\{(\eta^5\text{-}C_5H_3)_2(SiMe_2)_2\}Ru_2(CO)_4(H)(PR_3)]^+$ (**4a**−**b**). Reaction of $\mathbf{1}H^+BF_4^-$ and NaOMe in THF generates $\{(\eta^5\text{-}C_5H_4)_2SiMe_2\}Ru_2(CO)_4$ (**5**), resulting from the cleavage of a single $SiMe_2$ group, while the reaction of $\mathbf{1}H^+BF_4^-$ and NaOMe in MeOH generates $\{\mu\text{-}\eta^5{:}\eta^5\text{-}(C_5H_3SiMe_2OMe)(C_5H_4)SiMe_2\}Ru_2(CO)_4$ (**6**), resulting from the partial cleavage of a $SiMe_2$ group. Reaction of $\mathbf{1}H^+BF_4^-$ and NaSR (R = Me, Et) in THF generates $\{(\eta^5\text{-}C_5H_3)_2(SiMe_2)_2\}Ru_2(CO)_4(H)(SR)$ (R = Me, Et; **7a**−**b**), which undergoes rearrangement upon contact with neutral and basic alumina or silica to give complexes $\{\mu\text{-}\eta^5{:}\eta^1{:}\eta^5\text{-}(C_5H_3C{=}O)(C_5H_4)(SiMe_2)_2O\}Ru_2(\mu\text{-}SR)(CO)_3$ (R = Me, Et; **8a**−**b**). Molecular structures of **4a**, **6**, and **8a** as determined by X-ray diffraction studies are also presented.

Introduction

Nucleophilic attack on coordinated ligands is a reaction common to a number of transition metal complexes and constitutes a transformation of synthetic importance.[1] One of the simplest approaches to making a complex more positive, and thus more susceptible to nucleophilic attack, is to add a proton (H^+) to the metal center and/or the metal−metal bond.[2] However, most protonated metal complexes either do not undergo nucleophilic attack because they are not electrophilic enough, or basic nucleophiles, which are usually also good bases, simply deprotonate the metal to give the unreactive neutral metal complex. We recently reported[3] the synthesis of the cationic dinuclear complex $[\{(\eta^5\text{-}C_5H_3)_2(SiMe_2)_2\}Ru_2(CO)_4(\mu\text{-}H)]^+BF_4^-$ ($\mathbf{1}H^+BF_4^-$), whose carbon monoxide ligands are activated to nucleophilic attack by amines (eq 1) because of the positive charge on the complex and the relatively slow rate of deprotonation of the bridging hydride by the amines. In this paper, we report different types of reactions of $\mathbf{1}H^+BF_4^-$ with nucleophiles (halide anions, nucleophilic phosphines, ^-OMe, ^-SMe) to give a variety of new complexes. While the reaction in eq 1 illustrates amine attack on a CO ligand of $\mathbf{1}H^+BF_4^-$, the reactions in the present paper show that other nucleophiles add to the Ru or to the Si atom of the linking $(\eta^5\text{-}C_5H_3)_2(SiMe_2)_2$ ligand.

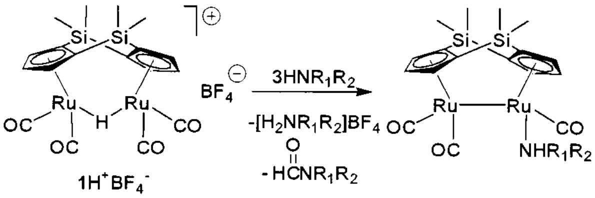

(1)

Scheme 1

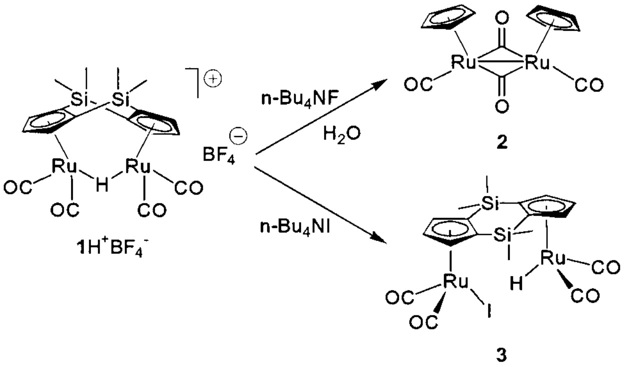

Results and Discussion

Reactions of $[\{(\eta^5\text{-}C_5H_3)_2(SiMe_2)_2\}Ru_2(CO)_4(\mu\text{-}H)]^+BF_4^-$ ($\mathbf{1}H^+BF_4^-$) with Halide Anions (n-Bu_4NX; X = F, Cl, Br, I). Synthesis of $\{(\eta^5\text{-}C_5H_3)_2(SiMe_2)_2\}Ru_2(CO)_4(H)(I)$ (3). Complex $\mathbf{1}H^+BF_4^-$ reacts with an excess of n-Bu_4NF in THF to give the simple $(\eta^5\text{-}C_5H_5)_2Ru_2(CO)_4$ (**2**)[4] complex (Scheme 1) as the only Ru-containing product. The reaction is very fast and exothermic. Presumably, this reaction proceeds by initial

---

* To whom correspondence should be addressed. E-mail: angelici@iastate.edu.

[†] Iowa State University, Molecular Structure Laboratory.

[‡] Current address: Department of Chemistry, University of Wisconsin, Madison, WI 53706.

(1) (a) McDaniel, K. F. In *Comprehensive Organometallic Chemistry*; Wilkinson, G., Stone F. G. A., Abel, E W., Eds.; Pergamon Press: Oxford, New York 1995; Vol. 12, p 601. (b) Collman, J. P.; Hegedus, L. S.; Norton, J. R.; Finke, R. G. *Principles and Applications of Organotransition Metal Chemistry*; University Science Books: Mills Valley, CA, 1987; Chapter 7. (c) Müller, T. E.; Beller, M. *Chem. Rev.* **1998**, *98*, 67.

(2) (a) Angelici, R. J. *Acc. Chem. Res.* **1995**, *28*, 52. (b) Kristjánsdóttir, S. S.; Norton, J. R. In *Transition Metal Hydrides: Recent Advances in Theory and Experiments*; Dedieu, A., Ed.; VCH: New York, 1991; Chapter 10. (c) Pearson, R. G. *Chem. Rev.* **1985**, *85*, 41. (d) Martinho Simões, J. A.; Beauchamp, J. L. *Chem. Rev.* **1990**, *90*, 629. (e) Bullock, R. M. *Comments Inorg. Chem.* **1991**, *12*, 1.

(3) (a) Ovchinnikov, M. V.; Angelici, R. J. *J. Am. Chem. Soc.* **2000**, *122*, 6130. (b) Ovchinnikov, M. V.; Guzei, I. A.; Angelici, R. J. *Organometallics* **2001**, *20*, 691.

(4) Doherty, N. M.; Knox, S. A. R.; Morris, M. J. *Inorg. Synth.* **1990**, *28*, 189.

10.1021/ic010644n CCC: \$20.00

F^- cleavage of the $SiMe_2$ groups followed by fast deprotonation of the protonated intermediate complex $[(\eta^5\text{-}C_5H_5)_2Ru_2(CO)_4(\mu\text{-}H)]^+$ by F^-. Water, which is present in and cannot be removed from the commercial solution of *n*-Bu_4NF in THF, serves as the proton source for this reaction. Formation of complex **2** is not surprising since F^- is a known reagent for the deprotection of silylated substrates;[5] the deprotonated complex $\{(\eta^5\text{-}C_5H_3)_2(SiMe_2)_2\}Ru_2(CO)_4$ (**1**) also reacts rapidly with *n*-Bu_4NF to give **2**.

Reactions of $\mathbf{1}H^+BF_4^-$ with Cl^- or Br^- proceed to give the deprotonated complex **1** as the only product at extremely slow rates ($t_{1/2} > 24$ h) at room temperature. On the other hand, reaction of $\mathbf{1}H^+BF_4^-$ with I^- gives within 24 h a 55% yield of $\{(\eta^5\text{-}C_5H_3)_2(SiMe_2)_2\}Ru_2(CO)_4(H)(I)$ (**3**) as a mildly air-sensitive solid (Scheme 1). The only other Ru-containing product is the deprotonated complex **1** (30%) resulting from the deprotonation of $\mathbf{1}H^+BF_4^-$ by I^-. The IR spectrum of **3** in hexanes solution shows the expected four strong ν(CO) absorptions of equal intensities corresponding to the $\{(\eta^5\text{-}C_5H_3)(SiMe_2)_2\}Ru(CO)_2(I)$ (2050, 2004 cm^{-1}) and $\{(\eta^5\text{-}C_5H_3)(SiMe_2)_2\}Ru(CO)_2(H)$ (2035, 1977 cm^{-1}) portions of the molecule; these assignments are based on a comparison with ν(CO) bands for $CpRu(CO)_2(I)$ (2048, 1997 cm^{-1})[6] and $CpRu(CO)_2(H)$ (2023, 1958 cm^{-1}).[4] The ^1H NMR spectrum of **3** at room temperature shows two sets of doublets and triplets in the range δ 5.34−5.91 for the protons of each cyclopentadienyl ring, which is consistent with two nonequivalent AB_2 spin systems. The Ru−H resonance occurs as a singlet at δ −10.84.

Reactions of $[\{(\eta^5\text{-}C_5H_3)_2(SiMe_2)_2\}Ru_2(CO)_4(\mu\text{-}H)]^+BF_4^-$ ($\mathbf{1}H^+BF_4^-$) with Phosphines (PEt_3, $PMePh_2$). Synthesis of $[\{(\eta^5\text{-}C_5H_3)_2(SiMe_2)_2\}Ru_2(CO)_4(H)(PR_3)]^+$ (4a,b). We reported[3] that the pK_a of $\mathbf{1}H^+BF_4^-$ could be determined by studying the proton-transfer reaction between PPh_3 and $\mathbf{1}H^+BF_4^-$. Over the course of these studies, we observed trace sideproducts that appeared to contain both η^1-H and η^1-PPh_3 ligands. Therefore, we sought to investigate the reactivity of $\mathbf{1}H^+BF_4^-$ with more nucleophilic and less bulky phosphines. When $\mathbf{1}H^+BF_4^-$ and PR_3 (PMe_3, PEt_3, PMe_2Ph, $PMePh_2$) are allowed to react in acetonitrile (5−50 min for PMe_3, PEt_3; 2−6 h for PMe_2Ph; and 6−48 h for $PMePh_2$), complexes $[\{(\eta^5\text{-}C_5H_3)_2(SiMe_2)_2\}Ru_2(CO)_4(H)(PR_3)]^+$ (**4a**,**b**; R_3 = $MePh_2$ (**a**), Et_3 (**b**)) are obtained in 95% yields as air-sensitive colorless crystalline solids (eq 2).

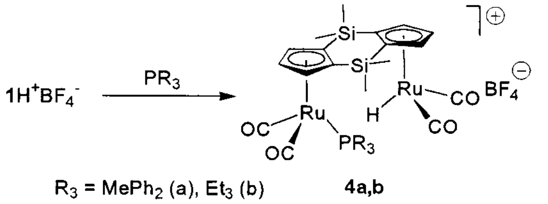

(2)

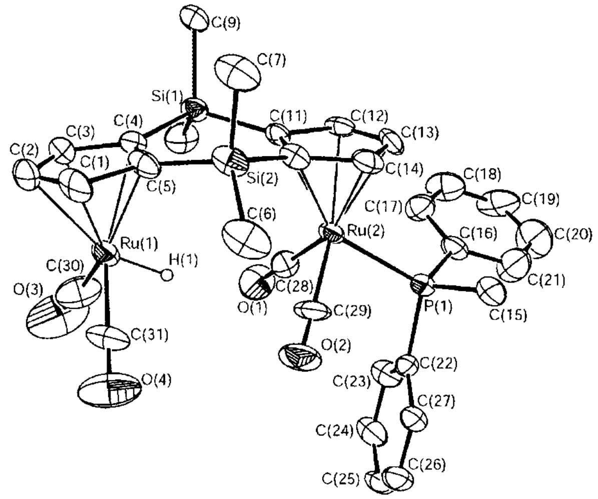

Figure 1. Thermal ellipsoid drawing of $[\{(\eta^5\text{-}C_5H_3)_2(SiMe_2)_2\}Ru_2(CO)_4(H)(PMePh_2)]^+$ (**4a**) showing the labeling scheme and 30% probability ellipsoids; hydrogens are omitted for clarity. Selected bond distances (Å) and angles (deg) are as follows: Ru(1)−Ru(2), 4.662(9); Ru(1)−C(30), 1.813(16); Ru(1)−C(31), 1.861(13); Ru(2)−C(28), 1.882(12); Ru(2)−C(29), 1.888(11); Ru(2)−P(1), 2.334(3); P(1)−C(15), 1.820(11); Ru(1)−Cp(centroid), 1.916(3); Ru(2)−Cp(centroid), 1.903(3); ∠C(30)−Ru(1)−C(31), 89.6(6); ∠C(28)−Ru(2)−C(29), 90.9(5); ∠C(28)−Ru(2)−P(1), 89.6(3); ∠C(29)−Ru(2)−P(1), 88.3(4); ∠Cp-(centroid)-Ru(1)−Ru(2)−Cp(centroid), 0.7; ∠Cp-Cp fold angle, 170.09.

Table 1. Crystallographic Data for **4a**, **6**, and **8a**

	4a	**6**	**8a**
formula	$C_{31}H_{32}BF_4O_4PRu_2Si_2\cdot 1/2CH_2Cl_2$	$C_{19}H_{22}O_5Ru_2Si_2$	$C_{19}H_{22}O_5Ru_2SSi_2$
fw	887.13	588.69	620.75
cryst syst	monoclinic	orthorhombic	triclinic
space group	$P2_1$	*Pbca*	$P\bar{1}$
a, Å	12.781(7)	16.7840(11)	10.5499(4)
b, Å	21.254(11)	13.2842(8)	14.3296(6)
c, Å	14.342(8)	19.9675(13)	16.4601(7)
α, deg	90	90	92.7868(10)
β, deg	104.886(9)	90	106.5317(10)
γ, deg	90	90	102.3499(10)
V, $Å^3$	3765(3)	4452.0(5)	2314.31(16)
Z	4	8	4
cryst color habit	colorless prism	orange prism	orange block
cryst size mm	0.40 × 0.20 × 0.20	0.30 × 0.30 × 0.20	0.40 × 0.30 × 0.30
μ(Mo Kα) mm^{-1}	1.032	1.491	1.526
temp, K	298(2)	298(2)	173(2)
abs cor	empirical	empirical	empirical
θ range	191−23.25°	2.37−26.37°	1.46−26.37°
no. of rflns collected	31150	24731	20646
no. of indep rflns	10786 [R(int) = 0.0694]	4556 [R(int) = 0.0289]	9379 [R(int) = 0.0161]
$R(F)^a$ $I \geq 2\sigma(I)$	R1 = 0.0527 wR2 = 0.1227	R1 = 0.0230 wR2 = 0.0535	R1 = 0.0201 wR2 = 0.0504

[a] $R1 = \sum||F_o| - |F_c||/\sum|F_o|$, $wR2 = \{\sum[w(F_o^2-F_c^2)^2]/\sum[w(F_o^2)^2]\}^{1/2}$.

Their IR spectra in CH_3CN solution show the expected four strong ν(CO) absorptions corresponding to the $[\{(\eta^5\text{-}C_5H_3)(SiMe_2)_2\}Ru(CO)_2(PR_3)]^{+,7}$ and $\{(\eta^5\text{-}C_5H_3)(SiMe_2)_2\}Ru(CO)_2(H)$ moieties. An X-ray structural determination of **4a** shows (Figure 1, Table 1) that the asymmetric unit contains two different molecules. In each of these molecules the Ru atoms exhibit a three-legged piano-stool geometry. The most interesting feature of the structure is the almost flat conformation of the $(\eta^5\text{-}C_5H_3)_2(SiMe_2)_2$ ligand (∠Cp−Cp fold angle = 170.09°), which is consistent with the long Ru−Ru nonbonding distance (4.662(9) Å). The cyclopentadienyl rings of the bridging ligand are not twisted with respect to each other, which is evident in the torsion angle ∠Cp(centroid)−Ru(1)−Ru(2)−Cp(centroid) (0.7°). Such a small twist may reflect the lack of steric repulsion between the cisoid $Ru(CO)_2H$ and $Ru(CO)_2(PMePh_2)$ units. The

---

(5) Greene, T. W.; Wuts, P. G. M. *Protective Groups in Organic Synthesis*; John Wiley & Sons: New York, 1999.

(6) Joseph, M. F.; Page, J. A.; Baird, M. C. *Organometallics* **1984**, *3*, 1749.

(7) Treichel, P. M.; Komar, D. A. *Synth. React. Inorg. Met.-Org. Chem.* **1980**, *10*, 205.

absence of the deprotonated complex **1** product in eq 2 indicates that the cleavage reactions are faster than the rates of deprotonation of **1**H$^+$BF$_4^-$ by phosphines. It is worth mentioning that the reaction completion times were inconsistent from run to run under identical experimental conditions and varied greatly for unknown reasons. Because of this, attempted kinetic studies of the reaction of **1**H$^+$BF$_4^-$ with PMePh$_2$ were unsuccessful. Presumably, these reactions are catalyzed by impurities or unidentified reaction sideproduct(s), which are not observed during the course of or at the end of the reaction.

The observed cleavage (Scheme 1 and eq 2) of the protonated Ru−Ru bond in [{(η^5-C$_5$H$_3$)$_2$(SiMe$_2$)$_2$}Ru$_2$(CO)$_4$(μ-H)]$^+$ (**1**H$^+$BF$_4^-$) by I$^-$ and phosphines is a relatively rare type of reaction. To the best of our knowledge, only one other example of this type of cleavage has been reported (eq 3).[8]

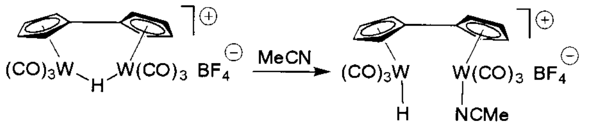

(3)

It involves a hydride-bridged fulvalene ditungsten complex, which reacts with acetonitrile to give the cleavage product. There was no reaction of the following potential ligands with **1**H$^+$BF$_4^-$ at room temperature within 24 h: pyridine, MeCN, C$_2$H$_4$, phenylacetylene.

Reactions of [{(η^5-C$_5$H$_3$)$_2$(SiMe$_2$)$_2$}Ru$_2$(CO)$_4$(μ-H)]$^+$BF$_4^-$ (1H$^+$BF$_4^-$) with NaOMe and NaSMe. Synthesis of {μ-η^5:η^5-(C$_5$H$_3$SiMe$_2$OMe)(C$_5$H$_4$)SiMe$_2$}Ru$_2$(CO)$_4$ (6) and {μ-η^5:η^1:η^5-(C$_5$H$_3$C=O)(C$_5$H$_4$)(SiMe$_2$)$_2$O}Ru$_2$(μ-SR)(CO)$_3$ (8a,b; R = Me, Et). It is well known[1a] that electropositive transition metal complexes undergo nucleophilic attack by alkoxide anions on coordinated alkene and CO ligands. In contrast, when complex **1**H$^+$BF$_4^-$ and NaOMe are reacted in THF for 10 min, {(η^5-C$_5$H$_4$)$_2$SiMe$_2$}Ru$_2$(CO)$_4$ (**5**) is obtained as the only isolated product, in 42% yield as an air-stable yellow crystalline solid (Scheme 2). Complex **5**, which was previously reported,[9] is readily identified by its IR spectrum (2005 (vs), 1966 (vs), 1936 (m), and 1758 (m) cm^{-1}) and the characteristic AA′BB′ (δ 5.66−5.06 ppm range) spin system in its ^{1}H NMR spectrum. It is unclear how this reaction proceeds from a mechanistic point of view since the formation of each molecule of **5** requires two protons and the starting complex, **1**H$^+$BF$_4^-$, can provide only one proton. Assuming the yield of **5** would be higher if the reaction were conducted in a protic medium, we investigated the reaction of **1**H$^+$BF$_4^-$ with NaOMe in MeOH solvent. Surprisingly, a mixture of **1** and the monolinked complex {μ-η^5:η^5-(C$_5$H$_3$SiMe$_2$OMe)(C$_5$H$_4$)SiMe$_2$}Ru$_2$(CO)$_4$ (**6**) was isolated in an approximately 1:2 ratio (Scheme 2). Complex **6**, which is isolated in 58% yield as yellow, air-sensitive crystals, was identified by the characteristic patterns in its ^{1}H NMR and IR spectra. The IR spectrum of **6** in hexanes shows ν(CO) absorptions at 2019 (vs), 2008 (s),1971 (s), 1950 (s), 1940 (m), and 1795 (m) cm^{-1}, which corresponds to both terminal and bridging CO ligands. The ^{1}H NMR spectrum of **6** exhibits resonances for the inequivalent “C$_5$H$_3$” and “C$_5$H$_4$” Cp rings (each displays a unique ABC and ABCD splitting pattern) and four signals for the Si(CH$_3$)$_2$ methyl groups in the δ 0.26−0.47 range. The δ 3.56 singlet is assigned to the MeO group.

Scheme 2

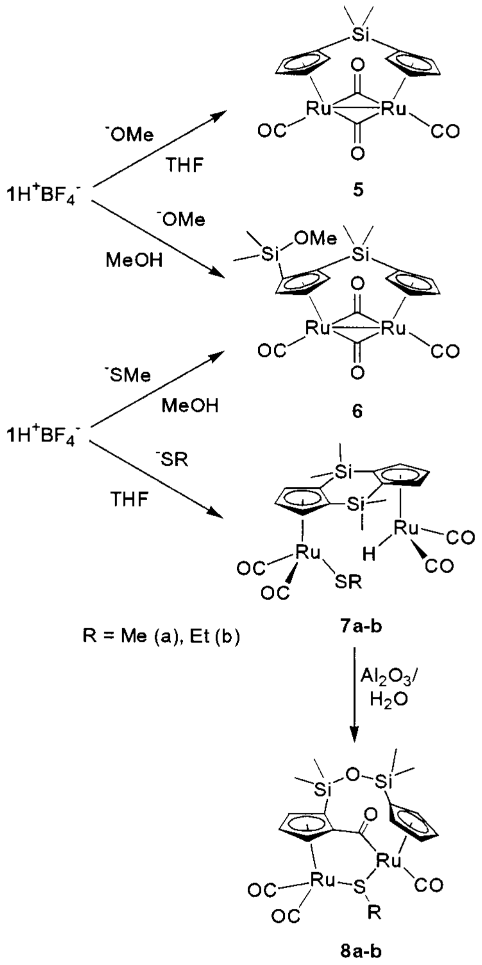

Although a detailed mechanism for the reaction of **1**H$^+$BF$_4^-$ with MeO$^-$ is undoubtedly complex, it presumably involves initial attack by the MeO$^-$ on a linking SiMe$_2$ group followed by proton transfer to the Cp ring.

A single-crystal X-ray structural determination (Figure 2, Table 1)[10] of **6** shows that the Ru−Ru distance in **6** (2.7049(3) Å) is the same as that (2.7042(4) Å) in complex **5**. In fact, both structures are almost identical in terms of the corresponding bond distances and angles. There is only a small twist around the Ru−Ru axis; this is reflected in the small ∠Cp(centroid)−Ru(1)−Ru(2)−Cp(centroid) torsion angle (8.0°).

Complex **1**H$^+$BF$_4^-$ reacts with NaSMe in MeOH to give the same products as those obtained from the reactions of **1**H$^+$BF$_4^-$ with NaOMe in MeOH, a mixture of complexes **1** (33%) and **6** (51%) in approximately the same 1:2 ratio. This observation suggests that MeO$^-$ acts as the nucleophile in both reactions. However, the reaction between **1**H$^+$BF$_4^-$ and NaSMe in THF leads to {(η^5-C$_5$H$_3$)$_2$(SiMe$_2$)$_2$}Ru$_2$(CO)$_4$(H)(SMe) (**7a**). Spectroscopic features of **7a** are similar to those of complex **3**. The ^{1}H NMR spectrum of **7a** exhibits resonances for the inequivalent Cp rings (each displays a unique AB$_2$ splitting pattern), two signals for the Si(CH$_3$)$_2$ methyl groups at δ 0.33 and 0.59, and a characteristic upfield signal for the hydride ligand at δ −10.66.

---

(8) Tilset, M.; Vollhardt, K. P. C.; Boese, R. *Organometallics* **1994**, *13*, 3146.

(9) Bitterwolf, T. E.; Leonard, M. B.; Horine, P. A.; Shade, J. E.; Rheingold, A. L.; Staley, D. J.; Yap, G. P. A. *J. Organomet. Chem.* **1996**, *512*, 11.

(10) Crystallographic data (excluding structure factors) for the structures in this paper have been deposited with the Cambridge Crystallographic Data Centre as supplementary publication no. CCDC-165288 (**4a**), no. CCDC-165287 (**6**), and no. CCDC-165286 (**8a**). Copies of the data can be obtained, free of charge, on application to CCDC, 12 Union Road, Cambridge CB2 1EZ, UK, (fax, +44 1223 336033; or e-mail, deposit@ccdc.cam.ac.uk).

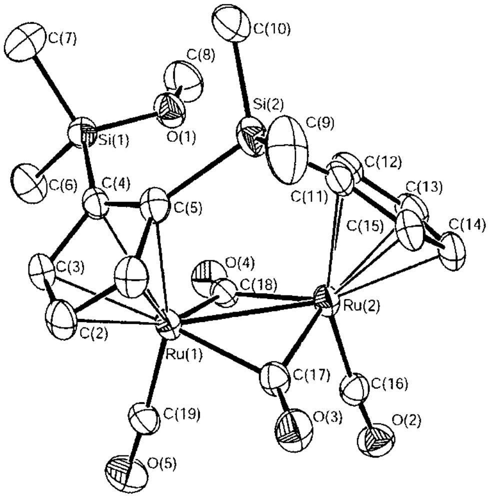

Figure 2. Thermal ellipsoid drawing of $\{\mu\text{-}\eta^5{:}\eta^5\text{-}(C_5H_3SiMe_2OMe)(C_5H_4)SiMe_2\}Ru_2(CO)_4$ (**6**) showing the labeling scheme and 30% probability ellipsoids; hydrogens are omitted for clarity. Selected bond distances (Å) and angles (deg) are as follows: Ru(1)−Ru(2), 2.7049(3); Ru(1)−C(19), 1.859(3); Ru(1)−C(17), 2.056(3); Ru(1)−C(18), 2.048(3); Ru(2)−C(16), 1.858(3); Ru(2)−C(17), 2.029(3); Ru(2)−C(18), 2.060(3); Ru(1)−Cp(centroid), 1.981(3); Ru(2)−Cp(centroid), 1.977(3); ∠C(19)−Ru(1)−C(17), 90.03(12); ∠C(19)−Ru(1)−C(18), 85.73(12); ∠C(17)−Ru(1)−C(18), 92.34(10); ∠Ru(1)−Ru(2)−C(16), 105.55(8); ∠Ru(2)−Ru(1)−C(19), 104.11(9); ∠Cp(centroid)−Ru(1)−Ru(2)−Cp(centroid), 8.0; ∠C(19)−Ru(1)−Ru(2)−C(16), 4.30(5); ∠Cp−Cp fold angle, 104.83.

The IR spectrum of **7a** in hexanes solutions shows the expected four strong ν(CO) absorptions of equal intensities corresponding to the $\{(\eta^5\text{-}C_5H_3)(SiMe_2)_2\}Ru(CO)_2(SMe)$ (2044, 1995 cm^{-1}) and $\{(\eta^5\text{-}C_5H_3)(SiMe_2)_2\}Ru(CO)_2(H)$ (2035, 1977 cm^{-1}) moieties. Attempts to isolate pure **7a** were unsuccessful due in part to the fact that this compound undergoes structural rearrangement on contact with neutral and basic alumina or silica during routine column chromatography to give complex **8a**. Complex **7b** undergoes the same transformation.

The structure of **8a** (Figure 3, Table 1) was conclusively established by an X-ray crystallographic analysis. The two ruthenium atoms are bridged by the μ-SMe group and by the $\{\mu\text{-}\eta^5{:}\eta^1{:}\eta^5\text{-}(C_5H_3C{=}O)(C_5H_4)(SiMe_2)_2O\}$ ligand, which binds in a η^5 fashion to Ru(1) and $\eta^5{:}\eta^1$ to Ru(2). The Ru(1)−S(1) and Ru(2)−S(1) distances are slightly different (2.3809(6) and 2.3450(6) Å); the μ-SMe ligand exhibits a trigonal-pyramidal geometry about the sulfur (pseudo-sp^3 hybridization). This geometry is indicated by the sum of the angles around the S atom (325.8°), which is considerably smaller than the 360° expected for an sp^2-hybridized sulfur. Both Ru atoms exhibit a three-legged piano-stool geometry with approximately 90°(±5°) angles between the noncyclopentadienyl ligands.

The IR spectrum of **8a** in hexanes shows ν(CO) absorptions at 2038 (vs), 1992 (vs), 1934 (m) cm^{-1}, which correspond to the three terminal CO ligands, and at 1591 (w) cm^{-1}, which is assigned to the acyl CO group. The ^1H NMR spectrum of **8a** exhibits seven resonances for the inequivalent Cp rings (they display unique ABC and ABCD splitting patterns), four signals for the $Si(CH_3)_2$ methyl groups in the δ 0.35−0.42 range, and a signal at δ 2.41 which corresponds to the μ-SMe group.

The observed conversion of **7** to **8** is a complicated transformation for which a mechanism is not obvious. Presumably, water on the alumina surface serves as the source of the oxygen atom for the construction of the $SiMe_2OSiMe_2$ link.

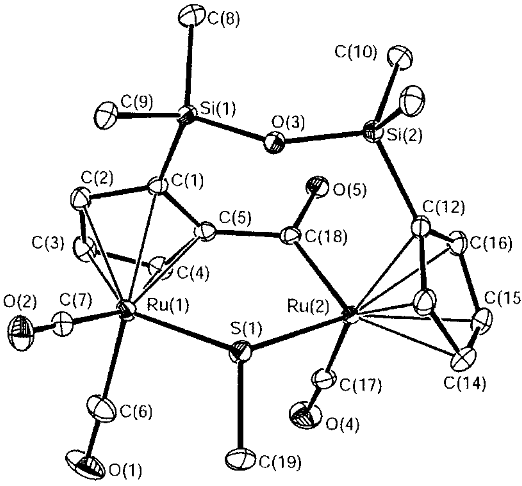

Figure 3. Thermal ellipsoid drawing of $\{\mu\text{-}\eta^5{:}\eta^1{:}\eta^5\text{-}(C_5H_3C{=}O)(C_5H_4)(SiMe_2)_2O\}Ru_2(\mu\text{-}SMe)(CO)_3$ (**8a**) showing the labeling scheme and 30% probability ellipsoids; hydrogens are omitted for clarity. Selected bond distances (Å) and angles (deg) are as follows: Ru(1)−Ru(2), 3.898(3); Ru(1)−S(1), 2.3809(6); Ru(2)−S(1), 2.3450(6); C(19)−S(1), 1.813(3); Ru(1)−C(7), 1.896(2); Ru(1)−C(6), 1.880(3); Ru(2)−C(17), 1.844(3); Ru(2)−C(18), 2.026(2); C(5)−C(18), 1.521(3); C(18)−O(5), 1.232(3); Ru(1)−Cp(centroid), 1.919(6); Ru(2)−Cp(centroid), 1.884(6); ∠C(6)−Ru(1)−C(7), 90.79(11); ∠C(6)−Ru(1)−S(1), 94.67(10); ∠C(7)−Ru(1)−S(1), 89.59(7); ∠C(17)−Ru(2)−C(18), 86.52(10); ∠C(17)−Ru(2)−S(1), 91.61(8); ∠C(18)−Ru(2)−S(1), 91.47(6); ∠C(5)−C(18)−Ru(2), 122.74(14); ∠O(5)−C(18)−Ru(2), 125.02(16); ∠Ru(1)−S(1)−Ru(2), 111.13(2); ∠Ru(1)−S(1)−C(19), 107.89(11); ∠Ru(2)−S(1)−C(19), 106.75(10).

Conclusions

The dinuclear ruthenium complex $[\{(\eta^5\text{-}C_5H_3)_2(SiMe_2)_2\}Ru_2(CO)_4(\mu\text{-}H)]^+BF_4^-$ ($\mathbf{1}H^+BF_4^-$) is activated to react with nucleophiles as a result of the bridging proton, which is kinetically slow to be deprotonated by bases/nucleophiles. As shown previously (eq 1), amines react with $\mathbf{1}H^+BF_4^-$ by attacking a CO ligand. On the other hand, I^-, RS^-, and phosphines add (Schemes 1, 2; eq 2) at one of the Ru centers, resulting in cleavage of the Ru−H−Ru bond. The final type of addition to $\mathbf{1}H^+BF_4^-$ is that exhibited by MeO^- and F^-, which results in cleavage of Si−C(cyclopentadienyl) bonds to give **6** and $(\eta^5\text{-}C_5H_5)_2Ru_2(CO)_4$. Except for the reaction with F^-, all of these types of reactions depend on the presence of the proton on the Ru−Ru bond (Scheme 1). The unprotonated $\{(\eta^5\text{-}C_5H_3)_2(SiMe_2)_2\}Ru_2(CO)_4$ (**1**) undergoes no reactions with these nucleophiles (except F^-) under the mild room-temperature conditions of these studies.

Experimental Section

General Procedures. All reactions were performed under an argon atmosphere in reagent grade solvents, using standard Schlenk or drybox techniques.[11] Hexanes, methylene chloride, and diethyl ether were purified by the Grubbs method prior to use.[12] All other solvents were purified by published methods.[13] Chemicals were purchased from Aldrich Chemical Co., unless otherwise mentioned, or prepared by literature methods, as referenced below. Alumina (neutral, activity I, Aldrich) was degassed under vacuum for 12 h and treated with Ar-saturated water (7.5% w/w). ^1H and ^{13}C NMR spectra were recorded

---

(11) Errington, R. J. *Advanced Practical Inorganic and Metalorganic Chemistry*, 1st ed; Chapman & Hall: New York, 1997.

(12) Pangborn, A. B.; Giardello, M. A.; Grubbs, R. H.; Rosen, R. K.; Timmers, F. J. *Organometallics* **1996**, *15*, 1518.

(13) Perrin, D. D.; Armarego, W. L. F.; Perrin, D. R. *Purification of Laboratory Chemicals*, 2nd ed; Pergamon: New York, 1980.

on a Bruker DRX-400 spectrometer using deuterated solvents as internal references. Solution infrared spectra were recorded on a Nicolet-560 spectrometer using NaCl cells with 0.1 mm spacers. Elemental analyses were performed on a Perkin−Elmer 2400 series II CHNS/O analyzer.

Reaction of $\mathbf{1H^+BF_4^-}$ with *n*-$\mathbf{Bu_4NF}$. A suspension of $\mathbf{1}$H$^+$BF$_4^-$ (10.0 mg, 15.5 μmol) in THF (50 mL) was treated with a solution of *n*-Bu$_4$NF in THF (0.2 mL, 1.0 M). The resulting orange solution contained mainly (η^5-C$_5$H$_5$)$_2$Ru$_2$(CO)$_4$ (**2**) as indicated by IR bands at 2005 (vs), 1966 (vs), 1936 (m), and 1758 (m) cm^{-1}, which are characteristic of **2**.[4]

Reaction of $\mathbf{1H^+BF_4^-}$ with *n*-$\mathbf{Bu_4NI}$. Synthesis of $\{(\eta^5\text{-C}_5\text{H}_3)_2\text{-(SiMe}_2)_2\}\text{Ru}_2(\text{CO})_4(\text{H})(\text{I})$ (3). A solution of **1**H$^+$BF$_4^-$ (50.0 mg, 77.5 μmol) and *n*-Bu$_4$NI (300 mg, 0.8 mmol) in CH$_2$Cl$_2$ (30 mL) was stirred for 24 h. Solvent was removed under vacuum; the resulting yellow residue was redissolved in hexanes/CH$_2$Cl$_2$ (10:1) (5 mL) and chromatographed on an alumina column (20 × 1 cm) with hexanes/CH$_2$Cl$_2$ (10:1) as the eluent. A yellow band was eluted and collected. Then, a dark-yellow band was eluted with hexanes/CH$_2$Cl$_2$ (4:1). From the first fraction, 13 mg (30%, based on **1**H$^+$BF$_4^-$) of **1** were obtained. From the second fraction, 29 mg (55%, based on **1**H$^+$BF$_4^-$) of pale yellow crystalline **3** were obtained. ^{1}H NMR (400 MHz, CDCl$_3$): δ −10.84 (s, 1 H, Ru-*H*), 0.36 (s, 6 H, Si(C*H*$_3$)), 0.57 (s, 6 H, Si(C*H*$_3$)), 5.34 (d, J = 2.4 Hz, 2 H, Cp), 5.55 (d, J = 2.4 Hz, 2 H, Cp), 5.77 (t, J = 2.4 Hz, 1 H, Cp), 5.91 (t, J = 2.4 Hz, 1 H, Cp). IR (hexanes): ν(CO) (cm^{-1}) 2050 (vs), 2035 (vs), 2004 (vs), 1977 (vs). Anal. Calcd for C$_{18}$H$_{19}$IO$_4$Ru$_2$Si$_2$·1/2CH$_2$Cl$_2$: C, 30.56; H, 2.77. Found: C, 30.95; H, 2.74.

Synthesis of $[\{(\eta^5\text{-C}_5\text{H}_3)_2(\text{SiMe}_2)_2\}\text{Ru}_2(\text{CO})_4(\text{H})(\text{PMePh}_2)]\text{BF}_4$ (4a). A yellow solution of **1**H$^+$BF$_4^-$ (120 mg, 0.19 mmol) and PMePh$_2$ (39 μL, 0.20 mmol) in CH$_3$CN (50 mL) was stirred for 6−20 h at ambient temperature. The reaction was followed by IR until the starting complex **1**H$^+$BF$_4^-$ disappeared. The resulting pale yellow solution was filtered through a short pad of Celite, and the filtrate was layered with Et$_2$O (200 mL) to precipitate (**4a**) as colorless crystals (149 mg, 95%). ^{1}H NMR (400 MHz, CD$_3$CN): δ −10.34 (s, 1 H, Ru-*H*), 0.39 (s, 6 H, Si(C*H*$_3$)), 0.60 (s, 6 H, Si(C*H*$_3$)), 2.44 (d, J = 10.8 Hz, 3 H, PC*H*$_3$), 5.70 (m, 5 H, Cp-*H*), 5.89 (t, J = 2.4 Hz, 1 H, Cp-*H*), 5.56 (m, 10 H, PPh$_2$). ^{31}P{^{1}H} NMR (162 MHz, CD$_3$CN): δ 30.68 (s, *P*MePh$_2$). IR (CH$_3$CN): ν(CO) (cm^{-1}) 2058 (vs), 2025 (vs), 2009 (vs), 1961 (vs). Anal. Calcd for C$_{31}$H$_{32}$BF$_4$O$_4$PRu$_2$Si$_2$·CH$_3$CN: C, 44.75; H, 3.98. Found: C, 44.59; H, 3.93. Crystals of **4a** suitable for X-ray diffraction analysis were obtained by slow cooling of a saturated solution of **4a** in Et$_2$O/CH$_2$Cl$_2$/MeCN (10:2:1) to −20 °C.

Synthesis of $[\{(\eta^5\text{-C}_5\text{H}_3)_2(\text{SiMe}_2)_2\}\text{Ru}_2(\text{CO})_4(\text{H})(\text{PEt}_3)]\text{BF}_4$ (4b). By reacting PEt$_3$ (19 μL, 0.17 mmol) with complex **1**H$^+$BF$_4^-$ (100 mg, 0.16 mmol) in CH$_3$CN (30 mL), **4b** (112 mg, 95%; colorless solid) was prepared and isolated using the same methods used for the preparation of **4a**. ^{1}H NMR (400 MHz, CD$_3$CN): δ −10.77 (s, 1 H, Ru-*H*), 0.39 (s, 6 H, Si(C*H*$_3$)), 0.59 (s, 6 H, Si(C*H*$_3$)), 1.13 (dt, J = 7.2, 20.8 Hz, 9 H, PCH$_2$C*H*$_3$), 2.07 (dq, J = 7.2, 9.6 Hz, 6 H, PC*H*$_2$-CH$_3$), 5.69 (d, J = 2.4 Hz, 2 H, Cp-*H*), 5.76 (d, J = 2.4 Hz, 2 H, Cp-*H*), 5.90 (t, J = 2.4 Hz, 1 H, Cp-*H*), 6.00 (m, 1 H, Cp-*H*). ^{31}P{^{1}H} NMR (162 MHz, CD$_3$CN): δ 47.52 (s, *P*Et$_3$). IR (CH$_3$CN): ν(CO) (cm^{-1}) 2052 (vs), 2024 (vs), 2001 (vs), 1961 (vs).

Reaction of $\mathbf{1H^+BF_4^-}$ with NaOMe. Method 1. Solid NaOMe (10.0 mg, 185 μmol) was added to a suspension of **1**H$^+$BF$_4^-$ (50.0 mg, 77.6 μmol) in THF (50 mL), and the mixture was stirred for 10 min. The resulting orange solution contained mainly {(η^5-C$_5$H$_4$)$_2$SiMe$_2$}Ru$_2$(CO)$_4$ (**5**), as indicated by IR bands at 2005 (vs), 1966 (vs), 1936 (m), and 1758 (m) cm^{-1}. After the solvent was removed under vacuum, the mixture was chromatographed on an alumina column (20 × 1 cm) first with hexanes and then with hexanes/CH$_2$Cl$_2$ (5:1), which eluted a yellow band containing **5** (17 mg, 42%). Its IR and ^{1}NMR spectra are the same as those previously reported[9] for this compound.

Method 2. Synthesis of $\{\mu\text{-}\eta^5\text{:}\eta^5\text{-(C}_5\text{H}_3\text{SiMe}_2\text{OMe)(C}_5\text{H}_4\text{)SiMe}_2\}\text{-Ru}_2(\text{CO})_4$ (6). Solid NaOMe (10.0 mg, 185 μmol) was added to a solution of **1**H$^+$BF$_4^-$ (50.0 mg, 77.6 μmol) in MeOH (50 mL), and the mixture was stirred for 10 min. Solvent was removed under vacuum; the resulting yellow residue was dissolved in hexanes (2 mL) and chromatographed on an alumina column (20 × 1 cm) with hexanes/CH$_2$Cl$_2$ (10:1) as the eluent. A yellow band was eluted and collected. Then, a second yellow band was eluted with hexanes/CH$_2$Cl$_2$ (5:1). From the first fraction, 12 mg (27%, based on **1**H$^+$BF$_4^-$) of **1** were obtained. From the second fraction, 26 mg (58%, based on **1**H$^+$BF$_4^-$) of pale yellow crystalline {μ-η^5:η^5-(C$_5$H$_3$SiMe$_2$OMe)(C$_5$H$_4$)SiMe$_2$}Ru$_2$(CO)$_4$ (**6**) were obtained. ^{1}H NMR (400 MHz, CDCl$_3$): δ 0.26 (s, 3 H, Si(C*H*$_3$)), 0.43 (s, 3 H, Si(C*H*$_3$)), 0.46 (s, 3 H, Si(C*H*$_3$)), 0.47 (s, 3 H, Si(C*H*$_3$)), 3.56 (s, 3 H, OC*H*$_3$), 5.22 (m, 1 H, Cp-*H*), 5.37 (m, 1 H, Cp-*H*), 5.60 (m, 1 H, Cp-*H*), 5.63 (m, 1 H, Cp-*H*), 5.71 (m, 1 H, Cp-*H*), 5.77 (m, 1 H, Cp-*H*), 5.82 (m, 1 H, Cp-*H*). ^{13}C NMR (100 MHz, CDCl$_3$): δ −2.55, −2.06, 0.02, 0.17 (*C*H$_3$), 49.71 (O*C*H$_3$), 84.72, 88.45, 89.13, 90.73, 91.18, 93.69, 95.99 100.59, 101.49, 104.31 (Cp), 216.36 (*C*O). IR (hexanes): ν(CO) (cm^{-1}) 2019 (vs), 2008 (s),1971 (s), 1950 (s), 1940 (m), 1795 (m). Anal. Calcd for C$_{19}$H$_{22}$O$_5$PRu$_2$Si$_2$: C, 36.83; H, 3.58. Found: C, 36.98; H, 4.01. Crystals of **6** suitable for X-ray diffraction analysis were obtained by slow cooling of a saturated solution of **6** in hexanes/CH$_2$Cl$_2$ (10:1) to −20 °C.

Reaction of $\mathbf{1H^+BF_4^-}$ with NaSMe. Method 1. Solid NaSMe (12.0 mg, 169 μmol) was added to a solution of **1**H$^+$BF$_4^-$ (50.0 mg, 77.6 μmol) in MeOH (50 mL), and the mixture was stirred for 10 min. The resulting orange solution contained mainly {μ-η^5:η^5-(C$_5$H$_3$SiMe$_2$OMe)-(C$_5$H$_4$)SiMe$_2$}Ru$_2$(CO)$_4$ (**6**) (see above) and **1**. After the solvent was removed under vacuum, the resulting yellow residue was dissolved in hexanes (2 mL) and chromatographed on an alumina column (20 × 1 cm) with hexanes/CH$_2$Cl$_2$ (10:1) as the eluent. A yellow band, containing **1** (14 mg, 33%, based on **1**H$^+$BF$_4^-$), was eluted and collected. Then, a second yellow band containing **6** (23 mg, 51%, based on **1**H$^+$BF$_4^-$) was eluted with hexanes/CH$_2$Cl$_2$ (5:1).

Method 2. Synthesis of $\{\mu\text{-}\eta^5\text{:}\eta^1\text{:}\eta^5\text{-(C}_5\text{H}_3\text{C}{=}\text{O)(C}_5\text{H}_4)(\text{SiMe}_2)_2\text{O}\}\text{-Ru}_2(\mu\text{-SMe})(\text{CO})_3$ (8a). Solid NaSMe (12.0 mg, 169 μmol) was added to a suspension of **1**H$^+$BF$_4^-$ (50.0 mg, 77.6 μmol) in THF (50 mL), and the mixture was stirred for 30 min. The resulting orange solution contained some **1** but mainly {(η^5-C$_5$H$_3$)$_2$(SiMe$_2$)$_2$}Ru$_2$(CO)$_4$(H)(SMe) (**7a**), as indicated by the IR (ν(CO) 2044 (vs), 2035 (vs), 1995 (vs), 1977 (vs) cm^{-1}) and ^{1}H NMR spectra (400 MHz, CDCl$_3$, δ −10.66 (s, 1 H, Ru-*H*), 0.33 (s, 6 H, Si(C*H*$_3$)), 0.59 (s, 6 H, Si(C*H*$_3$)), 2.03 (s, 3 H, SC*H*$_3$), 5.47 (d, J = 2.4 Hz, 2 H, Cp), 5.55 (m, 2 H, Cp), 5.97 (t, J = 2.4 Hz, 1 H, Cp), 5.99 (t, J = 2.4 Hz, 1 H, Cp)). After the solvent was removed under vacuum, the resulting orange−brown residue was dissolved in hexanes/CH$_2$Cl$_2$ (5:1) (2 mL) and chromatographed on an alumina column (20 × 1 cm) with hexanes/CH$_2$Cl$_2$ (10:1) as the eluent. A yellow band was eluted and collected. Then, an orange band was eluted with CH$_2$Cl$_2$/MeOH (5:1). From the first fraction, 9 mg (21%, based on **1**H$^+$BF$_4^-$) of **1** were obtained. From the orange fraction, 30 mg (62%, based on **1**H$^+$BF$_4^-$) of orange crystalline {μ-η^5:η^1:η^5-(C$_5$H$_3$C=O)(C$_5$H$_4$)(SiMe$_2$)$_2$O}Ru$_2$(μ-SMe)(CO)$_3$ (**8a**) were obtained. ^{1}H NMR (400 MHz, CDCl$_3$): δ 0.35 (s, 3 H, Si(C*H*$_3$)), 0.35 (s, 3 H, Si-(C*H*$_3$)), 0.42 (s, 6 H, Si(C*H*$_3$)), 2.41 (s, 3 H, SC*H*$_3$), 4.83 (m, 1 H, Cp-*H*), 4.86 (m, 1 H, Cp-*H*), 4.88 (m, 1 H, Cp-*H*), 4.95 (m, 2 H, Cp-*H*), 5.18 (m, 1 H, Cp-*H*), 5.80 (t, J = 2.0 Hz, 1 H, Cp-*H*). ^{13}C NMR (100 MHz, CDCl$_3$): δ 1.20, 1.84, 1.88, 3.54 (*C*H$_3$), 32.92 (S*C*H$_3$), 78.23, 80.17, 82.22, 84.23, 84.43, 84.69, 85.38, 101.71, 105.27 (Cp; 9 out of 10 peaks), 191.65, 197.72, 207.84 (*C*O), 254.72 (Cp-*C*=O). IR (hexanes): ν(CO) (cm^{-1}) 2038 (vs), 1992 (vs), 1934 (m), 1591 (w). Anal. Calcd for C$_{19}$H$_{22}$O$_5$Ru$_2$SSi$_2$: C, 36.76; H, 3.57. Found: C, 36.95; H, 3.71. Crystals of **8a** suitable for X-ray diffraction analysis were obtained by slow cooling of a saturated solution of **8a** in hexanes to −20 °C.

Synthesis of $\{\mu\text{-}\eta^5\text{:}\eta^1\text{:}\eta^5\text{-(C}_5\text{H}_3\text{C}{=}\text{O)(C}_5\text{H}_4)(\text{SiMe}_2)_2\text{O}\}\text{Ru}_2(\mu\text{-SEt})(\text{CO})_3$ (8b). By reacting NaSEt (14 mg, 0.17 mmol) with complex **1**H$^+$BF$_4^-$ (50 mg, 77.6 μmol), **8b** (27 mg, 54%; orange solid) was prepared and isolated using the same method used in the preparation of **8a**. ^{1}H NMR (400 MHz, CDCl$_3$): δ 0.35 (s, 3 H, Si(C*H*$_3$)), 0.36 (s, 3 H, Si(C*H*$_3$)), 0.42 (s, 3 H, Si(C*H*$_3$)), 0.43 (s, 3 H, Si(C*H*$_3$)), 1.09 (t, J = 7.2 Hz, 3 H, SCH$_2$C*H*$_3$), 2.63 (m, 2 H, SC*H*$_2$CH$_3$), 4.85 (m, 1 H, Cp-*H*), 4.90 (m, 3 H, Cp-*H*), 5.01 (m, 1 H, Cp-*H*), 5.13 (m, 1 H, Cp-*H*), 5.77 (m, 1 H, Cp-*H*). IR (hexanes): ν(CO) (cm^{-1}) 2036 (vs), 1990 (vs), 1934 (m), 1589 (w).

General Procedure for X-ray Structure Determinations. Data were collected on a Bruker CCD-1000 diffractometer. The structures were solved using direct methods and standard difference map techniques, and refined by full matrix least-squares procedures using SHELXTL.[14] All hydrogen atoms were placed in the structure factor calculation at idealized positions.

Acknowledgment. This work was supported by the National Science Foundation through Grant No. CHE-9816342.

Supporting Information Available: Complete details of the crystallographic study of **4a**, **6**, and **8a** (CIF). This material is available free of charge via the Internet at http://pubs.acs.org.

IC010644N

---

(14) All software and sources of the scattering factors are contained in the SHELXTL (version 5.1) program library (G. Sheldrick, Bruker Analytical X-ray Systems, Madison, WI).